

See discussions, stats, and author profiles for this publication at: <https://www.researchgate.net/publication/224131628>

Experimental investigations on the propagation of the plasma jet in the open air

Article in Journal of Applied Physics · May 2010

DOI: 10.1063/1.3369538 · Source: IEEE Xplore

CITATIONS

44

READS

112

13 authors, including:



Qing Xiong

Wuhan University

49 PUBLICATIONS 1,743 CITATIONS

SEE PROFILE



Xinpei Lu

Huazhong University of Science and Technology

170 PUBLICATIONS 6,465 CITATIONS

SEE PROFILE



Y. Xian

Huazhong University of Science and Technology

59 PUBLICATIONS 1,175 CITATIONS

SEE PROFILE



Chengwei Zou

Shandong University

28 PUBLICATIONS 963 CITATIONS

SEE PROFILE

Some of the authors of this publication are also working on these related projects:



NOx Fixation [View project](#)



plasma medicine [View project](#)

Experimental investigations on the propagation of the plasma jet in the open air

Q. Xiong, X. Lu,^{a)} Y. Xian, J. Liu, C. Zou, Z. Xiong, W. Gong, K. Chen, X. Pei, F. Zou, J. Hu, Z. Jiang, and Y. Pan

College of Electrical and Electronic Engineering, HuaZhong University of Science and Technology, WuHan, Hubei 430074, People's Republic of China

(Received 30 October 2009; accepted 23 February 2010; published online 12 April 2010)

The fundamental of the generation and propagation of the atmospheric pressure nonequilibrium plasma jets has recently attracted significant interests. In this paper, investigations on the effects of the parameters of the pulsed dc voltages on the optical emission intensity of the plasma jet and the bullet propagation behavior are carried out based on the temporal-spatial resolved optical emission spectroscopy measurements and the high-speed photography. It is found that, with the increase in the applied voltage, the bullet propagates out from the nozzle earlier and accelerates to higher peak-velocities. The increase in the pulse frequency exerts no significant influences on the optical emission of the plasma jet and the bullet propagation velocity. But it can induce the bullet propagates out from the nozzle earlier. Besides, it is interesting to notice that, with the increase in the pulse width in the beginning, the bullet propagates out from the nozzle with longer delay time. However, when the pulse width is increased to be more than 100 μs , the delay time of the bullet propagating out from the nozzle becomes much shorter. On the other hand, with the increase in the pulse width, the optical emission intensity of the plasma jet drops and the maximum bullet velocity decreases too. Detailed analysis shows that it may be due to the accumulation of the charges and radicals, which can shorten the prebreakdown of the discharge inside the syringe and result in the bullet propagating out earlier from the nozzle. © 2010 American Institute of Physics. [doi:10.1063/1.3369538]

I. INTRODUCTION

Atmospheric pressure nonequilibrium plasmas (APNPs) have been receiving widely attention for their attractive features, such as the ability to achieve enhanced plasma chemistry. This attractive characteristic made the APTNPs attractive in several practical applications, such as materials processing and synthesis,¹⁻³ surface modification,⁴ biomedical applications,⁵⁻⁸ chemical decontamination,^{9,10} water purification,¹¹⁻¹³ absorption and reflection of electromagnetic radiation.¹⁴ However, most traditional APTNPs sources generate stable plasmas either in a confined space between electrodes or contained inside a chamber, which indisputable leads inconveniences in the practical applications. Recently, the APNP jets (APNPJs) has attracted significant attentions, which is capable of addressing these concerns. The APNPJs devices are able to generate plasma plumes in the open space (surrounding air) rather than in confined discharge spaces.¹⁵⁻²² Some APNPJs devices can generate plasma plumes expanding into the surrounding air with a length of several centimeters or even longer, with gas temperature close to room-temperature.²³⁻²⁹ This characteristic is very important for the plasma medicine and increases the perspective of APNPJs in the biomedical applications, such as bacterial inactivation and root canal disinfection.³⁰⁻³⁴

Because of these attractive perspective applications mentioned above, the studies on the generation and propagation

mechanisms of the APNPJs have obtained growing interests. Recently we have reported a special designed single high-voltage (HV) electrode plasma jet device, which can generate plasma plume as long as 11 cm in the open air.²⁴ Some studies on this nonequilibrium atmospheric pressure plasma plume have been reported. High-speed photographs captured by intensified charge coupled devices (ICCDs) show that the plasma plume is not a continuous plasma but a fast-moving bulletlike plasma volumes, which is similar with other observations by other researchers with different devices.³⁵⁻⁴⁰ Further studies show that the plasma bullets are electrically driven,⁴¹ for which the photoionization mechanism may be responsible for the propagation of the bullets.³⁵ Detailed spatial-temporal resolved optical emission spectroscopy (OES) measurements reveal that the Penning effect between the metastable state He_m and the air molecules plays a significant role in the propagation of the plasma bullet in the open air.⁴² The plasma bullet reaches its peak-velocity while the emission intensity of the N_2^+ 391.4 nm line obtains its maximum. Meanwhile, the effects of the surrounding air, and various operational parameters, such as applied voltage, pulse width, and pulse repetition rate, on the length of the plasma jet were also investigated.⁴³ Although these preliminary progresses are obtained, many issues on the fundamental of the plasma jet remain unknown, such as why the jet length remains unchanged as the increase in the pulse frequency, why the length of the jet decreases when the pulse width is increased. All these issues need further detailed investigations.

^{a)}Author to whom correspondence should be addressed. Electronic mail: luxinpei@hotmail.com.

In this paper, the temporal resolved OES measurements and high-speed photographs are carried out to study the effects of the parameters of the pulsed dc voltages on the bullet behavior. It is found that the accumulation of the residual charges and reactive species may exert an influence on the consecutive discharge, which can induce the early ignition of the discharge and early appearance of the bullet from the nozzle. The rest of the paper is organized as follows. The experimental setup is described in Sec. II. Details of the experimental results, including the temporal resolved optical emission of the plasma jet and the spatial-temporal behavior of the bullet for the different discharge parameters, are presented in Sec. III. Section IV has a detailed discussion about the experimental results. Finally, Sec. V gives a brief summary of this work.

II. EXPERIMENTAL SETUP

The plasma jet studied in this paper is generated by a single HV electrode plasma device, which has been reported previously. Briefly, the plasma device is made of a medical glass syringe, inside which a HV electrode together with a quartz tube with one end closed are mounted. The HV electrode is made of a copper wire and inserted into the quartz tube. More detailed descriptions can be found in our previous reports.²⁷ The plasma device is driven by a pulsed dc power supply with amplitudes up to 10 kV, repetition rate up to 10 kHz, and pulse width variable from 200 ns to dc. Working gas such as He, Ar, or their mixtures with small amount of air can be used. In this paper, He gas with a flow rate of 2 l/min is used.

When high pulsed dc voltages are applied to the HV electrode and He gas is fed through the syringe, a homogeneous plasma jet is generated inside the syringe and in the surrounding air. In order to investigate the effects of various discharge parameters on the optical emission characteristics of the plasma jet and the bullet propagation behavior in the open air, the temporal resolved OES measurements and high-speed photography are carried out. The temporal resolved optical emission spectra are measured by a half meter spectrometer (Princeton Instruments Acton SpectraHub 2500i) and detected by an ICCD camera (Princeton Instruments, Model PIMAX2). The grating and the slit width of the spectrometer are set at 1200 groove/mm and 50 μm , respectively. The spatial resolution of the spectroscopic system is about 60 μm . The high-speed photographs are captured by the ICCD camera. For both the OES measurements and the high-speed photographs, the exposure time of the ICCD camera is set at 5 ns.

III. EXPERIMENTAL RESULTS

For all the experimental results in this paper, the flow rate of He gas is set at 2 l/min. The position along the axis of the plasma jet, from which the optical emission spectra is detected, is set at about 5 mm away from the nozzle outlet of the syringe. In this paper, four spectral lines are selected, i.e., N_2 ($\text{C } ^3\Pi_u, \nu_C=0 \rightarrow \text{B } ^3\Pi_g, \nu_B=0$) at 337.1 nm, N_2^+ ($\text{B } ^2\Sigma_u^+, \nu_B=0 \rightarrow \text{X } ^2\Sigma_g^+, \nu_X=0$) at 391.4 nm, He ($3\text{ } ^3\text{S}_1 \rightarrow 2\text{ } ^3\text{P}_{0,1,2}$) at 706.5 nm, and O ($3p\text{ } ^5\text{P} \rightarrow 3s\text{ } ^5\text{S}$) at 777.3 nm,

to study the optical emission characteristics of the plasma jet for different applied voltages V_a , pulse widths t_{pw} , and pulse frequencies f .

A. The influence of the applied voltage V_a

Figures 1(a)–1(d) shows the time evolution of the emission intensities of the four spectral lines for different applied voltages V_a . The onset of the applied voltages pulse is set as the zero time constant, as shown in Fig. 1(a), which is consistent for all the results presented in this paper as follows. As can be seen from Fig. 1, the emission of the four spectral lines performs a similar temporal behavior with the increase in V_a . They all increase and appear earlier when V_a is increased. For example, the N_2 337.1 nm line reaches its maximum intensity at about 0.84 μs for the V_a of 7 kV, and increases to a higher peak-value at 0.50 μs when V_a is increased to 9 kV. This observation is consistent with the dynamics of the plasma bullet when the V_a increases from 7 to 9 kV, as shown in Fig. 2. Figures 2(a) and 2(b) shows the temporal and spatial evolution of the bullet velocity for different V_a . The time delay of the appearance of the plasma bullet from the nozzle to the onset of V_a is also shown in Fig. 2(a). As can be seen, the bullet comes out from the nozzle earlier and propagates faster with higher applied voltages. The bullet can propagate in the open air with a peak-velocity of about 2.5×10^5 m/s when the V_a increases to 9 kV. Figure 2(b) shows the bullet velocities versus distance from the nozzle for different applied voltages. When the applied voltage increases, the bullet propagates to a longer distance with a higher speed and leads a longer plasma jet. This is consistent with the observation reported previously that a higher applied voltage could induce a longer length of the plasma jet.⁴³

B. The influence of the pulse width t_{pw}

The effect of the pulse width t_{pw} on the optical emission of the plasma jet is presented next. Figure 3 shows the temporal resolved emission intensity of the He 706.5 nm line for different pulse widths t_{pw} . It should be noted that the emission of the other spectral lines, i.e., N_2 337.1 nm, N_2^+ 391.4 nm, and O 777.3 nm have a similar temporal behavior with that of the He 706.5 nm line for different t_{pw} . As can be seen, the maximum emission intensity of the He 706.5 nm initially decreases as the t_{pw} increases. It is interesting to notice that, with the increase in the t_{pw} , He emission appears later. However, when t_{pw} is increased to be larger than 100 μs , this trend starts to change. When t_{pw} is increased to 150 μs , the He emission appears earlier than that t_{pw} of 100 μs . Besides, the He emission intensity is increased slightly. This temporal behavior becomes more obvious when t_{pw} is increased to be longer than 200 μs , as can be seen from Fig. 3 for the t_{pw} of 200 μs and 248 μs . It should be noticed that there is no change in the shape of the voltage pulse, and for other different pulse widths when a different repetition frequency of the voltage pulse is applied, the interesting transition is also present.

The influence of the pulse width on the bullet dynamics is shown in Figs 4(a) and 4(b). As the increase in the t_{pw} , the

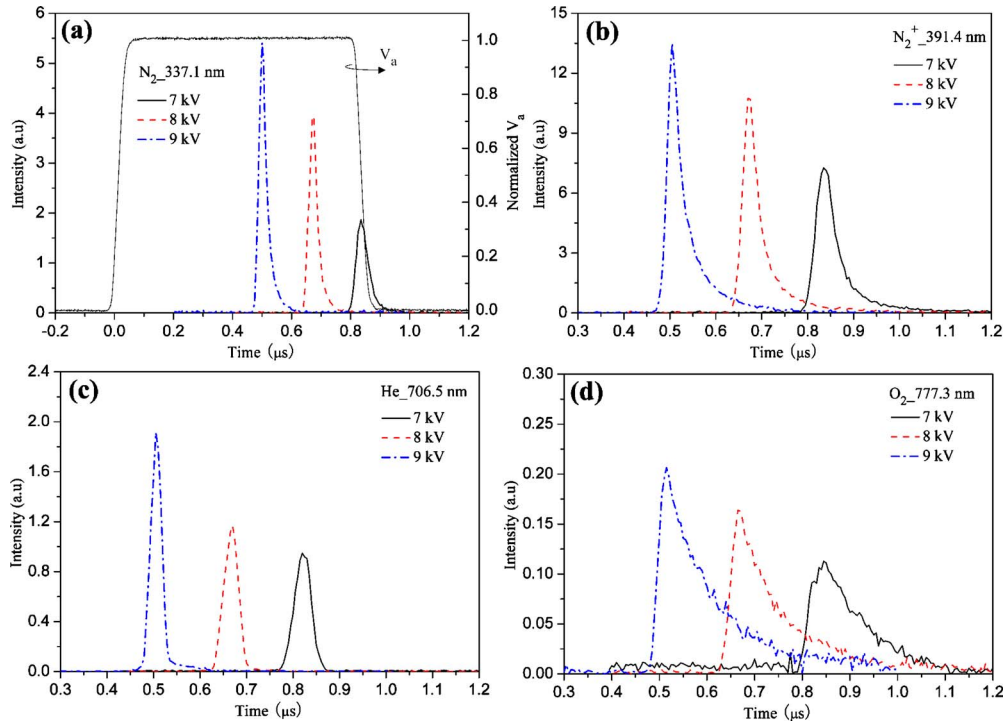


FIG. 1. (Color online) The temporal evolution of the emission at the (a) N_2 337.1 nm, (b) N_2^+ 391.4 nm, (c) He 706.5 nm, and (d) O 777.3 nm lines of the plasma jet for different applied voltages V_a , with $t_{pw}=800$ ns and $f=4$ kHz. In order to show the time delay between the onset of V_a and the detection of the optical emission, the normalized V_a is also presented in Fig. 1(a).

bullet comes out from the nozzle with longer delay time and its peak-velocity decreases [shown in Fig. 4(a)]. The bullet accelerates to its peak-velocity at a smaller distance away from the nozzle when the t_{pw} is increased to be longer [shown in Fig. 4(b)]. It should be noticed that the decay of the bullet velocity behaves more rapidly when the pulse width is short ($<0.8 \mu s$). As can be seen, the bullet velocity decreases rapidly after reaching its peak-value, although the bullet can accelerate to a large peak-velocity for the t_{pw} of $0.5 \mu s$. When the t_{pw} keeps rising to a large value (more than $100 \mu s$), however, the bullet starts to propagate out early and accelerates to a slightly higher peak-velocity at an advanced stage instead. This is similar with the temporal behavior of the He emission for different t_{pw} (shown in Fig. 3). In addition, the bullet reaches its peak-velocity at a slightly large distance from the nozzle when the t_{pw} becomes wider. A further increase in the t_{pw} (more than $200 \mu s$) has an adverse effect on the bullet propagation, which leads a decrease in the bullet velocity, although the bullet propagates out at a much earlier stage. When the t_{pw} rises to $248 \mu s$, the bullet cannot travel out from the nozzle and no plasma jet is generated in the open air. More discussion on this observation will also be given in Sec. IV.

C. The influence of the pulse frequency f

Figure 5 shows the effect of the pulse frequency f (repetition rate) on the temporal behaviors of the emission intensities of the four spectral lines. Because the emission intensity of the O 777.3 nm is much weaker than that of the other three lines, the temporal evolution of the O emission for different f is shown in the inset figure in Fig. 5. The pulse

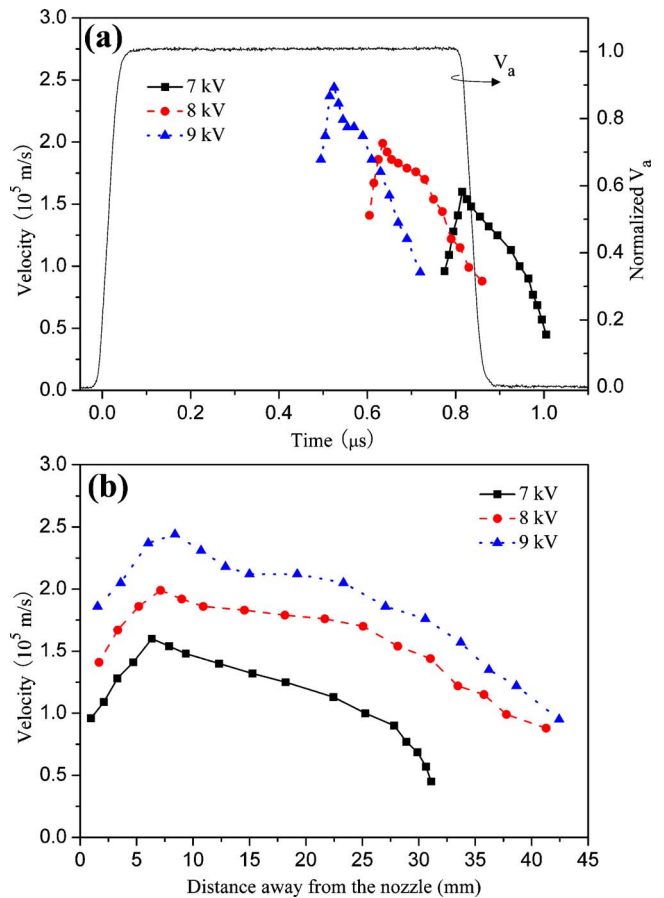


FIG. 2. (Color online) The (a) temporal and (b) spatial evolution of the bullet velocity for different applied voltages V_a , with $t_{pw}=800$ ns and $f=4$ kHz. In order to show the time delay between the onset of V_a and the appearance of the plasma bullet from the nozzle, the normalized V_a is also presented in Fig. 2(a).

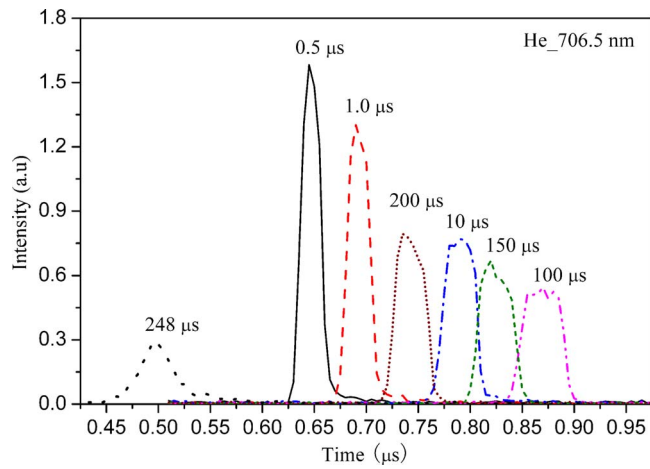


FIG. 3. (Color online) The time evolution of the emission at the He 706.5 nm line of the plasma jet for different pulse widths t_{pw} , with $V_a=8$ kV and $f=4$ kHz.

frequency is varied from 1 to 10 kHz. As can be seen, the pulse frequency does not affect the emission intensities significantly. On the other hand, it is worthwhile to note that the emission of the four lines appear much earlier for higher frequencies. This is consistent with the temporal behavior of the bullet velocity for different f , as shown in Fig. 6(a). The bullet propagates out from the nozzle much earlier for high pulse repetition rates. But the bullet almost propagates to a

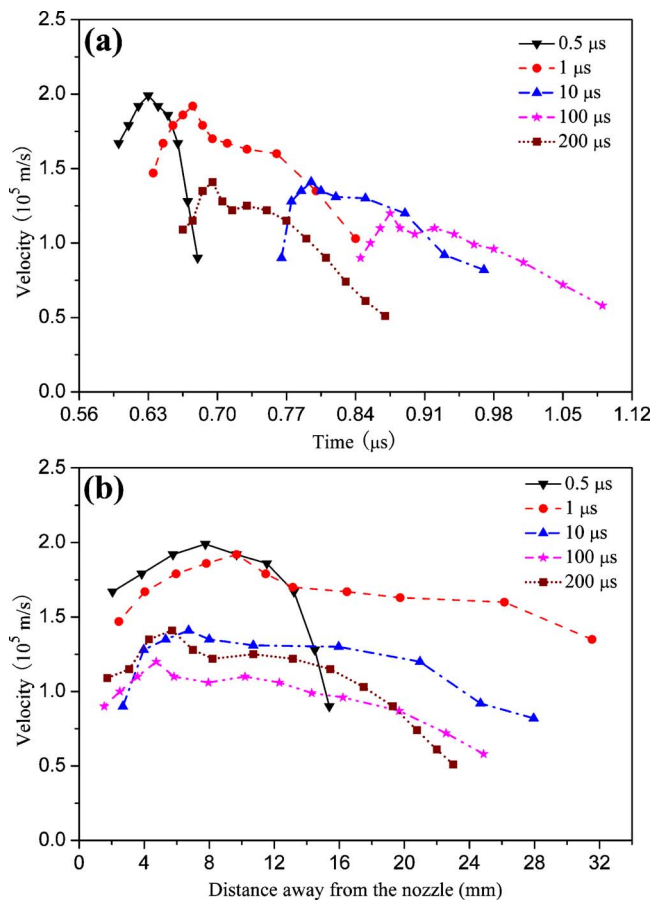


FIG. 4. (Color online) The (a) temporal and (b) spatial evolution of the bullet velocity for different pulse widths t_{pw} , with $V_a=8$ kV and $f=4$ kHz.

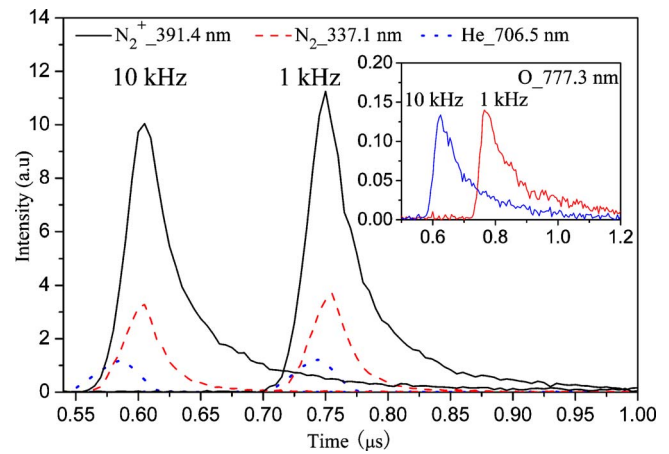


FIG. 5. (Color online) The time evolution of the emission at the N_2 337.1 nm (dashed), N_2^+ 391.4 nm (solid), He 706.5 nm (dotted), and O 777.3 nm (inset image) lines of the plasma jet for the pulse frequencies of 1 and 10 kHz, with $V_a=8$ kV and $t_{pw}=800$ ns.

same distance in the open air and accelerates to a peak-velocity about 2×10^5 m/s at the same position when f varies from 0.1 to 10 kHz, as shown in Fig. 6(b).

IV. DISCUSSION

A higher applied voltage can reduce the prebreakdown phase and induce an early ignition of the discharge inside the

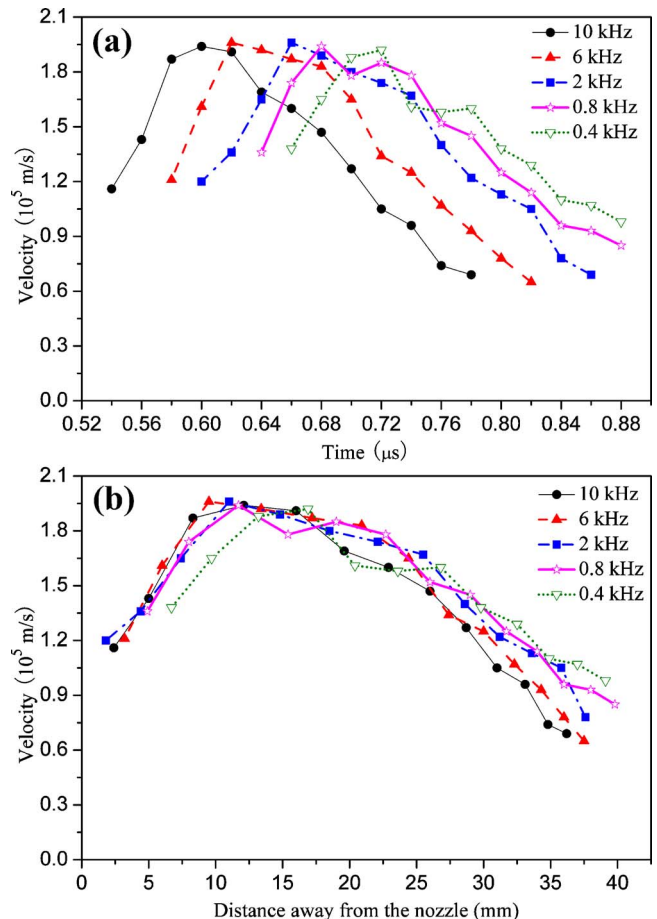


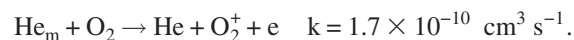
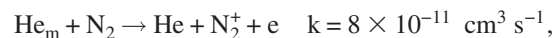
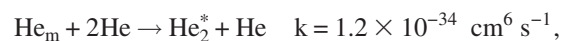
FIG. 6. (Color online) The (a) temporal and (b) spatial evolution of the bullet velocity for different pulse frequencies f , with $V_a=8$ kV and $t_{pw}=800$ ns.

syringe.^{16,43} Accordingly, the plasma bullet propagates out from the nozzle early and the optical emission is detected at an early stage. The plasma bullet propagates to a higher peak-velocity may be related to the larger quantity of charges generated during the positive discharge inside the syringe according to the photoionization-based plasma bullet model.³⁵ The essential of this model is that sufficient charges are required for sustaining the propagation of the ionization front of the plasma bullet. The more charges carried by the bullet, the faster the bullet propagates. More excited species are generated to emit strong optical emission through transitions from upper levels to lower levels.

The bullet propagates out from the nozzle at an early stage when f is increased. This may be attributed to early ignition of the discharge inside the syringe. More reactive species, such as $N_2 W^3\Delta_u$ and $W^1\Delta_u$, which have lifetimes between 0.1 and 10 ms comparable to the duration of the pulse off cycle, are accumulated inside the syringe when f is increased.⁴⁴ The larger amount of these reactive species may be effective in shortening the prebreakdown phase by producing more electrons and radicals through collision-reactions, and eventually induce the early appearance of the plasma bullet.

The situation is also similar for the cases with large pulse widths. The increase in the pulse width indicates the decrease in the voltage-off duration. For the pulse repetition rate of 4 kHz (pulse-cycle of 250 μ s), more reactive species with a relative long lifetime probably accumulate inside the syringe when the pulse width is much larger (more than 100 μ s), and reduce the prebreakdown phase of the consecutive discharge and result in the early appearance of the plasma bullet. However, we ignored the effect of the charged particles on the early ignition of discharges induced by the next voltage pulse-cycle due to the fast bulk recombination mechanism. As known that, when pure helium is used as working gas, the dominant ions are He^+ and He_2^+ ions. Due to the air impurity, high concentration of N_2^+ , O_2^+ , and O_2^- ions may also be present in the discharge inside the syringe. The negative O_2^- ions are mainly produced through the fast electron attachment because of the electronegative feature of O_2 molecules. In the absence of the external electric field, these charged particles, including the electrons, will perform a fast decay through fast electron-ion and ion-ion recombination. As we reported in Ref. 30, the peak electron density of the discharge was estimated in the order of 10^{13} cm^{-3} . And if the electron-ion recombination coefficient $\beta=10^{-7}$ $cm^3 s^{-1}$, the characteristic decay time of charged particles is estimated to be about 10^{-6} s.⁴⁵ Therefore, in our cases (normally duration of voltage-off is larger than 10 μ s), the density of charged particles should be very low at the moment the next voltage pulse being applied and not affect the prebreakdown phase of the consecutive discharge significantly.

Furthermore, the helium metastables He_m neither plays an important role in shortening the prebreakdown phase of the consecutive discharge in our cases because of its short lifetime. During the afterglow period of the discharge inside the syringe, the quenching mechanism of the helium metastables He_m is mainly due to the following fast reactions:⁴⁶



The latter two quenching reactions are known as the Penning ionization between the He_m and the air molecules. The high energy of the He_m (19.8 eV) is easy to transfer to the air molecules with relative low ionization potential, such as N_2 (15.6 eV) and O_2 (12.07 eV). The presence of the air molecules is because of the impurity of the helium working gas and the air diffusion from the syringe nozzle. The purity of the helium gas we used is 99.99%, therefore, the impurity will be more than 100 ppm due to the air diffusion from the open space. The lifetime of He_m is estimated to be less than 10 μ s due to the three quenching reactions mentioned above. So for our cases (pulse width less than 200 μ s for the frequency of 4 kHz), the density of He_m should also be low when the next voltage pulse is applied and not affect seriously in shortening the prebreakdown of the consecutive discharge. This can also be indicated from the very short duration of the intensity pulse of the emission line $N_2^+ 391.4$ nm during the positive discharge inside the syringe, during which the Penning ionization is important for the generation of the excited N_2^+ .⁴² But for the cases with very large pulse width more than 240 μ s (voltage-off duration less than 10 μ s), the He_m and the charged particles may have a residual density for the short voltage-off duration and influence the ignition of the consecutive discharge.⁴⁷

However, the interpretation mentioned above does not suitable for the case of the rise of the pulse width in the beginning (from submicroseconds to about 100 μ s), for which the bullet propagates out with a longer time delay and the optical emission of the plasma jet decreases initially. This interesting observation needs further detailed investigations.

V. CONCLUSION

In summary, the effects of the operational parameters, i.e., applied voltage V_a , pulse width (voltage-on duration) t_{pw} , pulse frequency (repetition rate) f , on the temporal resolved emission behaviors of the plasma jet and the bullet propagation in the open air have been studied. It is found that the applied voltage and pulse width exert significantly stronger influences on the optical emission characteristics of the plasma jet and the bullet dynamics than the pulse frequency. As the increase in the V_a , the optical emission is detected earlier with higher intensity, and the plasma bullet propagates out from the nozzle at an earlier stage and propagates to a larger peak-velocity. However, the rise of the pulse width has an adverse effect on the optical emission of the plasma jet and the bullet propagation. The bullet propagates out later with a lower peak-velocity initially as the voltage pulse becomes wider. However, further increasing the pulse width (more than 100 μ s), the bullet starts to appear early instead with a still low peak-velocity, which is more obvious when the voltage pulse width is increased to be close to dc signal. Detailed analysis shows that it may be due to the accumulation of the charges and radicals, which can shorten

the prebreakdown of the discharge inside the syringe and result in the bullet propagating out earlier from the nozzle. The variation in the pulse frequency does not affect the optical emission characteristics of the plasma jet and the bullet propagation noticeably, but a large pulse frequency can induce an earlier appearance of the plasma bullet from the nozzle.

ACKNOWLEDGMENTS

This work was supported in part by the National Natural Science Foundation under Grant No. 10875048 and in part by the Chang Jiang Scholars Program, Ministry of Education, People's Republic of China.

- ¹P. Chu, *IEEE Trans. Plasma Sci.* **35**, 181 (2007).
- ²K. Ostrikov, S. Kumar, and H. Sugai, *Phys. Plasmas* **8**, 3490 (2001).
- ³K. Ostrikov, *Rev. Mod. Phys.* **77**, 489 (2005).
- ⁴R. Dorai and M. Kushner, *J. Phys. D* **36**, 666 (2003).
- ⁵G. Fridman, G. Friedman, A. Gutsol, A. Shekhter, V. Vasilets, and A. Fridman, *Plasma Processes Polym.* **5**, 503 (2008).
- ⁶M. Laroussi, *Plasma Processes Polym.* **2**, 391 (2005).
- ⁷G. Fridman, A. Brooks, M. Galasubramanian, A. Fridman, A. Gutsol, V. Vasilets, H. Ayan, and G. Friedman, *Plasma Processes Polym.* **4**, 370 (2007).
- ⁸F. Iza, G. Kim, S. Lee, J. K. Lee, J. Walsh, Y. Zhang, and M. Kong, *Plasma Processes Polym.* **5**, 322 (2008).
- ⁹Z. Machala, E. Marode, M. Morvova, and P. Lukac, *Plasma Processes Polym.* **2**, 152 (2005).
- ¹⁰C. Jiang, A. H. Mohamed, R. H. Stark, J. H. Yuan, and K. H. Schoenbach, *IEEE Trans. Plasma Sci.* **33**, 1416 (2005).
- ¹¹Z. Machala, I. Jedlovsky, L. Chladekova, B. Pongrac, D. Giertl, M. Janda, L. Sikurova, and P. Polcic, *Eur. Phys. J. D* **54**, 195 (2009).
- ¹²P. Bruggeman, J. Liu, J. Degroote, M. Kong, J. Vierendeels, and C. Leys, *J. Phys. D* **41**, 215201 (2008).
- ¹³P. Bruggeman and C. Leys, *J. Phys. D* **42**, 053001 (2009).
- ¹⁴R. Vidmar, *IEEE Trans. Plasma Sci.* **18**, 733 (1990).
- ¹⁵M. Laroussi and T. Akan, *Plasma Processes Polym.* **4**, 777 (2007).
- ¹⁶J. Walsh and M. Kong, *Appl. Phys. Lett.* **91**, 221502 (2007).
- ¹⁷G. Li, H. Li, L. Wang, S. Wang, H. Zhao, W. Sun, X. Xing, and C. Bao, *Appl. Phys. Lett.* **92**, 221504 (2008).
- ¹⁸D. Mariotti, *Appl. Phys. Lett.* **92**, 151505 (2008).
- ¹⁹J. Walsh and M. Kong, *Appl. Phys. Lett.* **93**, 111501 (2008).
- ²⁰D. Kim, J. Rhee, B. Gweon, S. Moon, and W. Choe, *Appl. Phys. Lett.* **91**, 151502 (2007).
- ²¹E. Stoffels, Y. Sakiyama, and D. Graves, *IEEE Trans. Plasma Sci.* **36**, 1441 (2008).
- ²²Q. Nie, C. Ren, D. Wang, and J. Zhang, *Appl. Phys. Lett.* **93**, 011503 (2008).
- ²³M. Laroussi and X. Lu, *Appl. Phys. Lett.* **87**, 113902 (2005).
- ²⁴X. Lu, Z. Jiang, Q. Xiong, Z. Tang, X. Hu, and Y. Pan, *Appl. Phys. Lett.* **92**, 081502 (2008).
- ²⁵Z. Cao, J. Walsh, and M. Kong, *Appl. Phys. Lett.* **94**, 021501 (2009).
- ²⁶A. Shashurin, M. Keidar, S. Bronnikov, R. Jurjus, and M. Stepp, *Appl. Phys. Lett.* **93**, 181501 (2008).
- ²⁷X. Lu, Z. Jiang, Q. Xiong, Z. Tang, and Y. Pan, *Appl. Phys. Lett.* **92**, 151504 (2008).
- ²⁸Y. Hong and H. Uhm, *Appl. Phys. Lett.* **89**, 221504 (2006).
- ²⁹X. Zhang, J. Huang, X. Liu, L. Peng, L. Guo, G. Lv, W. Chen, K. Feng, and S. Yang, *J. Appl. Phys.* **105**, 063302 (2009).
- ³⁰X. Lu, T. Ye, Y. Cao, Z. Sun, Q. Xiong, Z. Tang, Z. Xiong, J. Hu, Z. Jiang, and Y. Pan, *J. Appl. Phys.* **104**, 053309 (2008).
- ³¹J. Lim, H. Uhm, and S. Li, *Phys. Plasmas* **14**, 093504 (2007).
- ³²J. Goree, B. Liu, and D. Drake, *J. Phys. D* **39**, 3479 (2006).
- ³³J. Kolb, A. Mohamed, R. Price, R. Swanson, A. Bowman, R. Chiavarini, M. Stacey, and K. Schoenbach, *Appl. Phys. Lett.* **92**, 241501 (2008).
- ³⁴X. Lu, Y. Cao, P. Yang, Q. Xiong, Z. Xiong, Y. Xian, and Y. Pan, *IEEE Trans. Plasma Sci.* **37**, 668 (2009).
- ³⁵X. Lu and M. Laroussi, *J. Appl. Phys.* **100**, 063302 (2006).
- ³⁶A. Shashurin, M. Shneider, A. Dogariu, R. Miles, and M. Keidar, *Appl. Phys. Lett.* **94**, 231504 (2009).
- ³⁷M. Teschke, J. Kedzierski, E. Finantu-Dinu, K. Korzec, and J. Engemann, *IEEE Trans. Plasma Sci.* **33**, 310 (2005).
- ³⁸B. Sands, B. Ganguly, and K. Tachibana, *Appl. Phys. Lett.* **92**, 151503 (2008).
- ³⁹R. Ye and W. Zheng, *Appl. Phys. Lett.* **93**, 071502 (2008).
- ⁴⁰N. Mericam-Bourdet, M. Laroussi, A. Begum, and E. Karakas, *J. Phys. D* **42**, 055207 (2009).
- ⁴¹X. Lu, Q. Xiong, Z. Xiong, J. Hu, F. Zhou, W. Gong, Y. Xian, C. Zhou, Z. Tang, Z. Jiang, and Y. Pan, *J. Appl. Phys.* **105**, 043304 (2009).
- ⁴²Q. Xiong, X. Lu, J. Liu, Y. Xian, Z. Xiong, F. Zou, C. Zou, W. Gong, J. Hu, K. Chen, X. Pei, Z. Jiang, and Y. Pan, *J. Appl. Phys.* **106**, 083302 (2009).
- ⁴³Q. Xiong, X. Lu, K. Ostrikov, Z. Xiong, Y. Xian, F. Zhou, C. Zou, J. Hu, W. Gong, and Z. Jiang, *Phys. Plasmas* **16**, 043505 (2009).
- ⁴⁴A. Lofthus and P. Krupenie, *J. Phys. Chem. Ref. Data* **6**, 113 (1977).
- ⁴⁵R. Yuri, *Gas Discharge Physics* (Springer-Verlag, New York, 1991).
- ⁴⁶G. Myers and A. Cunningham, *J. Chem. Phys.* **67**, 3352 (1977).
- ⁴⁷X. Lu, Q. Xiong, Z. Xiong, Y. Xian, F. Zhou, J. Hu, W. Gong, C. Zhou, Z. Tang, Z. Jiang, and Y. Pan, *IEEE Trans. Plasma Sci.* **37**, 647 (2009).